

Composition and Style Attributes Guided Image Aesthetic Assessment

Luigi Celona*, Marco Leonardi*[†], Paolo Napoletano*, and Alessandro Rozza[†]

*Department of Informatics, Systems and Communication, University of Milano-Bicocca, viale Sarca, 336
Milano, Italy

[†]lastminute.com, Corso S. Gottardo, 30 Chiasso, Switzerland

Abstract—The aesthetic quality of an image is defined as the measure or appreciation of the beauty of an image. Aesthetics is inherently a subjective property but there are certain factors that influence it such as, the semantic content of the image, the attributes describing the artistic aspect, the photographic setup used for the shot, etc. In this paper we propose a method for the automatic prediction of the aesthetics of an image that is based on the analysis of the semantic content, the artistic style and the composition of the image. The proposed network includes: a pre-trained network for semantic features extraction (the Backbone); a Multi Layer Perceptron (MLP) network that relies on the Backbone features for the prediction of image attributes (the AttributeNet); a self-adaptive Hypernetwork that exploits the attributes prior encoded into the embedding generated by the AttributeNet to predict the parameters of the target network dedicated to aesthetic estimation (the AestheticNet). Given an image, the proposed multi-network is able to predict: style and composition attributes, and aesthetic score distribution. Results on three benchmark datasets demonstrate the effectiveness of the proposed method, while the ablation study gives a better understanding of the proposed network.

Index Terms—Image aesthetic assessment, Image composition, Image style, Hypernetworks.

I. INTRODUCTION

AESTHETICS of an image is defined as the measure or appreciation of the beauty of an image. Image aesthetics is a subjective property that depends on the viewer’s preferences, experiences, and photography skills. Despite this, the occurrence of specific factors or patterns objectively makes an image more appealing than others. Researchers have in fact found that aesthetics can be influenced by several factors including lighting [1], color scheme [2], contrast [3], composition [4], semantic photo content [5], [6], and image styles [7], [8].

The semantic content of a photo is a key aspect in the evaluation of aesthetic quality: (i) psychology research shows that certain kinds of content are more attractive than others [9]; (ii) professional photographers choose different photographic techniques and have different aesthetic criteria in mind when shooting different types of contents [6], [10].

In the same way, image styles such as “Long Exposure”, “Macro”, “Bokeh” and others, or image geometric composition rules such as “Rule of Thirds”, “Curved” and others, influence the aesthetic quality of an image [7], [8]. Figure 1

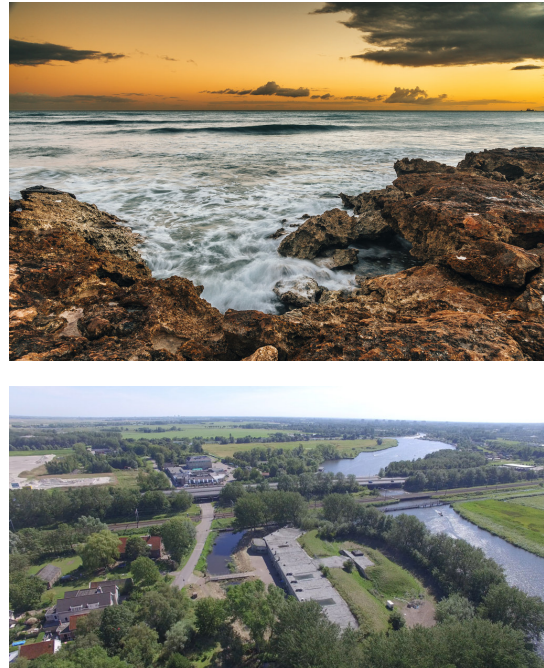


Fig. 1. Two images with high and low esthetics from the AADB database [11]. The top image has a high aesthetic likely thanks to good lighting and harmonious color combinations, while the image with a low aesthetic has low light and dull colors.

shows an example of a high-quality image (top) and a low-quality image (bottom). In this example, the image on the top has been rated on average by a group of humans with high level of aesthetics. This is likely due to nice attributes such as, good lighting and harmonious color combinations, which make the image attractive. In contrast, the image below has a low aesthetic level rate which likely is due to low light and dull colors.

Literature reports mostly on three different aesthetics recognition tasks: high vs. low aesthetic quality [4], [12]–[14], aesthetic score regression [15]–[18], and aesthetic score distribution prediction [19]–[21]. Whatever is the recognition task, most of researchers do not explicitly model the aforementioned factors that influence image aesthetics and indeed they prefer holistic approaches [6], [10], [16], [22]. Besides, methods explicitly modeling aesthetic attributes try to learn a universal model to be applied to images with different aesthetic attributes [17], [18], [23]. However, images that share the same

aesthetic attribute or particular combinations of attributes can also have different levels of aesthetics. It is therefore necessary to learn aesthetic prediction models that specialize for each type of attribute and at the same time are able to consider the correlation between several attributes.

In this work, we describe a new method that aims to resolve the aforementioned limitations. The proposed method models the aesthetics of the image by explicitly taking into account image semantic content, style and composition. In particular, we exploit side information related to aesthetic attributes in a way that each attribute is suitably employed to build an *ad-hoc* image aesthetics estimator.

To better exploit side information given by image style and composition attributes, the training stage of the proposed method is multi-stage. The first training stage involves a Multi Layer Perceptron (MLP) network (the AttributeNet) which is specially trained to recognize image style and composition. This network takes as input semantic features extracted by a pre-trained network (the Backbone). The second training stage concerns a hypernetwork (HyperNet). The latter exploits the attributes prior encoded into the embedding generated by the AttributeNet to predict the parameters of the target network dedicated to aesthetic estimation (AestheticNet). The adoption of the attribute-conditioned hypernetwork, therefore, determines attribute-specific aesthetic estimators. The HyperNet is trained using the Earth Mover's Distance (EMD) as a loss function to better learn the distribution of user judgments attributed to each image. This strategy allows to model the consensus and the diversity of opinions among the annotators and consequently to improve the effectiveness of the proposed method.

Given a test image, the proposed method predicts image style and composition as well as the aesthetic score distribution.

To summarize, the contribution of this work are the following.

- We present a deep learning-based method that not only it estimates aesthetics in terms of score distribution but it also determines the style and composition of the input image.
- We propose a hypernetwork which adaptively generates the aesthetic quality prediction parameters basing on aesthetic attributes. The proposed method predicts image aesthetics in a content- and attribute- aware manner, therefore it is not limited to a holistic evaluation of the aesthetic quality.
- We conduct comprehensive experiments for unified aesthetic prediction tasks: aesthetic classification, aesthetic regression, and aesthetic label distribution. For all of these tasks, the proposed method achieves higher performance than state-of-the-art approaches on three common benchmark datasets (AADB [11], AVA [24], and Photo.net [10]).

The reminder of this article is organized as follows. In Section II, related works are summarized. Section III defines the proposed attribute-guided aesthetic assessment method, that is then detailed in Section IV. Section V presents the datasets used for aesthetic-related attribute recognition as well

as those for aesthetic assessment. Section VI describes the evaluation and the training procedures. Section VII reports the quantitative evaluation of the proposed method and the comparison with previous methods. Finally, in Section VIII conclusions and future work are drawn.

II. RELATED WORKS

In this section, we review relevant literature related to image aesthetic quality assessment and we highlight the differences between the proposed method and similar existing methods.

A. Image aesthetic quality assessment

From the seminal work of Datta *et al.* [10] many research efforts have been made, and various methods have been proposed for estimating the aesthetics of images [25]. Several papers proposed the use of hand-crafted features to encapsulate both aspects of human perception and photographic rules. For example, Datta *et al.* [10] carefully selected 56 hand-crafted visual features based on standard photographic rules (such as rule of thirds, colorfulness, or saturation) to discriminate between aesthetically pleasing and displeasing images. Luo *et al.* [6] extracted features encoding photographic rules, e.g. composition, lighting, and color arrangement, to evaluate aesthetics in different ways based on the photo content. Zhang *et al.* [26] modeled image aesthetics by focusing on the image composition which is modeled using graphlets small-sized connected graphs.

However, methods based on hand-crafted features can only achieve limited success [25]: (i) hand-crafted features can not exhaustively model the variations of photographic rules between different categories of images; (ii) hand-crafted features are heuristics, and so it is challenging to mathematically model some photographic rules. Based on the previous considerations and thanks to the availability of more labeled data, the trend has shifted from hand-crafted feature-based methods to deep learning methods [15], [27], [28].

RAPID [12] is a double-column network that captures both local and global information of images for discriminating low and high aesthetics. Given that one patch may not well represent the fine-grained information in the entire image, Lu *et al.* [29] extended RAPID by proposing Deep Multi-patch Aggregation Network (DMA-Net). In DMA-Net, an input image is represented by a bag of random cropped patches. The proposed layers, namely the statistics and sorting layers, enabled the integration of multiple input patches. Given that DMA-Net failed to encode the global layout of the image, Ma *et al.* presented the Adaptive Layout-Aware Multi-Patch Convolutional Neural Network (A-Lamp CNN) [14]. This method is able to accept arbitrary sized images and learn from both fined grained details and holistic image layout simultaneously. It consists of two subnets, i.e. a Multi-Patch subnet which is very similar to DMA-Net and a Layout-Aware subnet consisting of an object-based attribute graph. Multi-Net Adaptive Spatial Pooling ConvNet (MNA-CNN) [30] is trained and tested on images at their original sizes and aspect ratios. It computed aesthetics by combining multi-level features and scene information. Chen *et al.* [21] designed the

Adaptive Fractional Dilated Convolution (AFDC) that, similarly to MNA-CNN, avoids altering original image aspect ratio and composition. RGNet [4] builds a region graph to represent the visual elements and their spatial layout in the image, and then performs reasoning on the graph to uncover the mutual dependencies of the local regions. Gated Peripheral-Foveal Convolutional Neural Network (GPF-CNN) [20] is a deep architecture designed to: encode the global image composition; extract the fine-grained details from aesthetic-relevant regions.

Professional photographers adopt different photographic techniques and have various aesthetic criteria depending on the portrait content. Therefore, Kao *et al.* [13] proposed a Multi-task Convolutional Neural Network (MTCNN). This model aims to simultaneously estimate the semantic content and the aesthetic class of an image.

Neural Image Assessment (NIMA) [19] replaced the classification layer of a pre-trained ImageNet CNN with a fully-connected regression head that predicts the distributions of ratings per image. The squared Earth Mover’s Distance (EMD) has been employed as the loss function. In this paper, similar with [19], we optimize our network for aesthetic score distribution by minimizing EMD loss. Multi-level Spatially Pooled activation blocks (MLSP) [16] exploited a transfer learning strategy that uses features extracted from a pre-trained ImageNet CNN.

Some recent works regard multi-modal aesthetic evaluation models that leverage visual information along with user comments. The latter encodes high-level semantic information and are relevant for aesthetic decisions [27], [28], [31].

B. Correlation with existing methods

There are several state-of-the-art methods similar to the one proposed in this article as they use multiple attributes describing the aesthetic or artistic aspect of a photo for aesthetic evaluation [11], [17], [18], [23], [32], [33].

Leonardi *et al.* [23] and Gao *et al.* [32] used attributes as mid-level representation to estimate the aesthetics of the image. Thus, the errors on the attributes might be propagated to the assessed aesthetics. Likewise, Lee *et al.* [33] presented the Property-Specific Aesthetic Assessment (PSAA) algorithm. The PSAA algorithm first classifies an image into a specific aesthetic property and then discriminates the image into a high or low aesthetic quality through a specific-property network. Our work differs from the PSAA in three main aspects. First, PSAA discriminates high or low aesthetics while we face the more challenging task of estimating the distribution of aesthetic scores. Second, the aesthetic categorization of PSAA depends exclusively on the aesthetic classifier for the specific property with the highest score, while our aesthetic estimate relies on the representation of the attributes and their interactions. Third, PSAA’s attribute estimation errors might be propagated to the assessed aesthetic, similarly as in the methods of Leonardi *et al.* and Gao *et al.* Pan *et al.* [18] proposed a multi-task deep network to learn the aesthetic score and aesthetic attributes simultaneously. Attributes were used as additional information for the learning paradigm called Learning Using Privileged Information (LUPI) [34]. Besides,

adversarial learning was introduced to capture the correlation between the aesthetic score and attributes. Shu *et al.* [17] also exploited LUPI by proposing Deep Convolutional Neural Network with Privileged Information (PI-DCNN): a novel method exploring photo attributes as privileged information for photo aesthetic assessment.

There are three major differences between the previous methods and the one proposed in this article which are summarized as follows:

- First, previous methods are limited to the datasets annotated with aesthetic attributes, namely AVA or AADB. In contrast, in the proposed method, side information about composition and style is learned from specially designed datasets. The proposed method can therefore generalize to a larger number of aesthetic attributes.
- Second, the previous methods learn a universal model of aesthetics that depends indiscriminately on the aesthetic attributes. In contrast, the proposed method learns aesthetic models that are dependent on the different aesthetic attributes present within the image and their correlation.
- Finally, we use Earth Mover’s Distance (EMD) as a loss function to better learn the distribution of user judgments attributed to each image. As demonstrated in previous works [19], [21], this strategy allows to model the consensus and the diversity of opinions among the annotators and consequently to improve the effectiveness of the proposed method.

III. PROPOSED METHOD

In the following we introduce the mathematical formulation of the proposed method. Given an input image \mathbf{X} , the goal of the proposed method is to estimate both the aesthetic score distribution $\hat{\mathbf{q}}$ and the presence of a set of aesthetic-related attributes $\hat{\mathbf{y}}$ by using the network f parametrized with θ^* :

$$\mathbf{X} \xrightarrow{f(\theta^*)} (\hat{\mathbf{q}}, \hat{\mathbf{y}}). \quad (1)$$

More specifically, $f \leftarrow (f_s, f_t)$ consists of two networks. The network f_s handles the *side* information regarding the aesthetic-related attributes and produces the final output $\hat{\mathbf{y}}$ and the embedding \mathbf{e}_s . The latter is exploited by an *attribute-conditioned* hypernetwork $\hat{\theta}_t = h(\mathbf{e}_s; \theta_h^*)$ that adaptively generate the parameters $\hat{\theta}_t$ of the network f_t . Such a network f_t carries out the *main* task of aesthetic assessment. Hence, by using the attribute-conditioned hypernetwork we subordinate the aesthetic assessment task to that of attribute estimation.

$\theta^* \leftarrow (\theta_h^*, \theta_s^*, \theta_b^*)$ is the set of learned parameters of the proposed method. Unlike the θ_b^* parameters, which belong to a pre-trained backbone, the others are learned for our tasks. Similar to [35], we adopt a two-step optimization procedure to introduce attribute-constraint into the hypernetwork.

The first step regards the training of the parameters θ_s of the network f_s . Let $\mathcal{D}_s = \{(\mathbf{X}_s^{(i)}, \mathbf{y}^{(i)})\}_{i=1}^N$ denotes the training set of N training samples. Each training sample consists of a color image $\mathbf{X}_s^{(i)} \in \mathbb{R}^d$ and K aesthetic-related attributes $\mathbf{y}^{(i)} \in \mathbb{R}^K$. Given the training set \mathcal{D}_s , our goal is to learn a

network $f_s : \mathbb{R}^d \rightarrow \mathbb{R}^K$, which predicts whether an attribute occurs or not into the input image:

$$\mathcal{L}_{side}\{f_s(\mathbf{e}_b; \theta_s, \mathbf{y}) \mid \theta_s \in \Theta_s\}, \quad (2)$$

where $\theta_s \in \Theta_s$ are the learnable real-valued parameters and $\mathbf{e}_b = b(\mathbf{X}_s; \theta_b^{*(L)})$ is the embedding corresponding to the activations of layer L of the pre-trained backbone b given the input \mathbf{X}_s .

The second training concerns the hypernetwork. Instead of directly learning the θ_t parameters of the network f_t , the hypernetwork is trained to learn the parameters θ_h of a metamodel h . The output of this metamodel is $\hat{\theta}_t$. The network h can therefore be thought of as a generator of parameters to obtain attribute-specific aesthetic estimators. Let $\mathcal{D}_t = (\mathbf{X}_t^{(i)}, \mathbf{q}^{(i)})_{i=1}^N$ denotes the training set of N training samples. Each training sample consists of a color image $\mathbf{X}_t^{(i)} \in \mathbb{R}^d$ and a distribution of aesthetics ratings $\mathbf{q}^{(i)} = [q_{s_1}, q_{s_2}, \dots, q_{s_B}]$. Where s_j is the j -th score bucket, B is the total number of score buckets, and q_{s_j} denotes the number of voters that give the discrete score s_j to the image. Given the training set \mathcal{D}_t , our goal is to learn the parameters θ_h of the metamodel to generate the parameters for the network $f_t : \mathbb{R}^d \rightarrow \mathbb{R}^B$, which predicts the aesthetic score distribution $\hat{\mathbf{q}}$:

$$\mathcal{L}_{task}\{f_t(\mathbf{e}_b; h(\mathbf{e}_s; \theta_h), \mathbf{q}) \mid \theta_h \in \Theta_h\}, \quad (3)$$

where \mathbf{e}_b is the same embedding as in Eq. 2, $\mathbf{e}_s = f_s(\mathbf{e}_b; \theta_s^{*(M)})$ is the attribute-conditioned embedding obtained from the M -th layer of the pre-trained f_s given the input \mathbf{e}_b , and $\theta_h \in \Theta_h$ are the learnable real-valued parameters.

IV. PROPOSED NETWORK ARCHITECTURES

The proposed architecture includes four different networks trained using a multi-stage approach: the Backbone, the AttributeNet, the HyperNet and the AestheticNet. The overall architecture of the model is shown in Figure 2.

The Backbone is an ImageNet [36] pre-trained neural network that outputs multi-level features used as inputs of the AestheticNet and the AttributeNet. The latter is a Multi Layer Perceptron (MLP) network specially trained for image style and composition recognition. The features obtained from the previously trained AttributeNet are then used as HyperNet inputs. It is a metamodel dedicated to calculating the weights and distortions of the AestheticNet. Therefore, the HyperNet is trained to allow the AestheticNet to predict aesthetics scores for input images in close agreement with human judgments.

The following sections detail each of the aforementioned components of the proposed method.

A. Backbone

Many of the earlier approaches to image aesthetics assessment extract features from warped and/or cropped input images [15], [17], [19]. A shortcoming of these methods is that they alter the composition of the image and the aspect ratio of the objects. Thus, they may harm the task of aesthetics assessment.

On the other hand, previous works have shown the effectiveness of multi-level features to predict perceptual judgements, either for image quality assessment [37] or image aesthetics assessment [16], [23], [38].

For the previous reasons, the Backbone network $b : \mathbf{X} \rightarrow \mathbf{e}_b$ encodes an input image, at the original size, $\mathbf{X} \in \mathbb{R}^d$ into a Multi-Level Spatially Pooled (MLSP) embedding vector $\mathbf{e}_b \in \mathbb{R}^D$. The resulting embedding vector encodes information at multiple levels of abstraction: from low- to high-level features. This goal is achieved by stacking activations from L layers of a given pre-trained CNN. As the spatial resolution of the different activation maps varies, a Global Average Pooling (GAP) is adopted to squeeze the spatial dimensions into a channel activation vector. Therefore, the size of the MLSP embedding vector depends solely on the number of channels in each layer. This last aspect allows processing images at full resolution without the need to resize or crop them.

To summarize, the Backbone network $b(\mathbf{X}; \theta_b^{*(L)})$ outputs the embedding \mathbf{e}_b corresponding to the activations of L layers given the input \mathbf{X} .

We exploit an ImageNet-pretrained EfficientNet-B4 [39] as Backbone network b : a very efficient yet effective model not only on ImageNet but also on transfer learning datasets. Recently, it demonstrates its effectiveness for image aesthetic assessment [23], [38]. Following [38], the activations of the MBConv blocks [39] having numbers $L = \{15, 21, 25, 29, 31\}$ are considered. Given the input image \mathbf{X} with shape $h \times w \times 3$, the resulting activation maps have the following shapes: $\frac{h}{16} \times \frac{w}{16} \times 112$, $\frac{h}{16} \times \frac{w}{16} \times 160$, $\frac{h}{32} \times \frac{w}{32} \times 272$, $\frac{h}{32} \times \frac{w}{32} \times 272$, and $\frac{h}{32} \times \frac{w}{32} \times 448$. The previous 5 activation maps are spatially narrowed using the GAP and stacked on the channel dimension, thus obtaining a fixed sized narrow MLSP embedding vector of shape $1 \times 1 \times 1264$.

B. AttributeNet

The AttributeNet $f_s : \mathbf{e}_b \rightarrow \hat{\mathbf{y}}$ with $\hat{\mathbf{y}} \in \mathbb{R}^K$ is a Multi Layer Perceptron (MLP) that aims to categorize the backbone embedding \mathbf{e}_b with respect to K aesthetic-related attributes. More specifically, $\hat{\mathbf{y}} \leftarrow (\hat{\mathbf{y}}_v, \hat{\mathbf{y}}_c)$, where $\hat{\mathbf{y}}_v \in \mathbb{R}^{K_v}$ is the set of image styles and $\hat{\mathbf{y}}_c \in \mathbb{R}^{K_c}$ is the set of composition rules. Therefore, the MLP performs two tasks simultaneously and consists of three linear blocks. The first block is a linear layer with ReLU that transforms the embedding vector \mathbf{e}_b into an embedding vector, \mathbf{e}_s :

$$\mathbf{e}_s = \text{ReLU}(\mathbf{W}_s^\top \mathbf{e}_b + \mathbf{b}_s). \quad (4)$$

Given that \mathbf{e}_s is shared between the two tasks, it intrinsically encodes the style and composition as well as their relationships. The second and third blocks are independent linear layers categorizing the input image into style and composition:

$$\hat{\mathbf{y}}_v = \mathbf{W}_v^\top \mathbf{e}_s + \mathbf{b}_v, \quad (5)$$

$$\hat{\mathbf{y}}_c = \mathbf{W}_c^\top \mathbf{e}_s + \mathbf{b}_c, \quad (6)$$

where \mathbf{W}_v and \mathbf{b}_v are the parameters for predicting the style $\hat{\mathbf{y}}_v$, and \mathbf{W}_c and \mathbf{b}_c are the parameters for predicting the composition $\hat{\mathbf{y}}_c$.

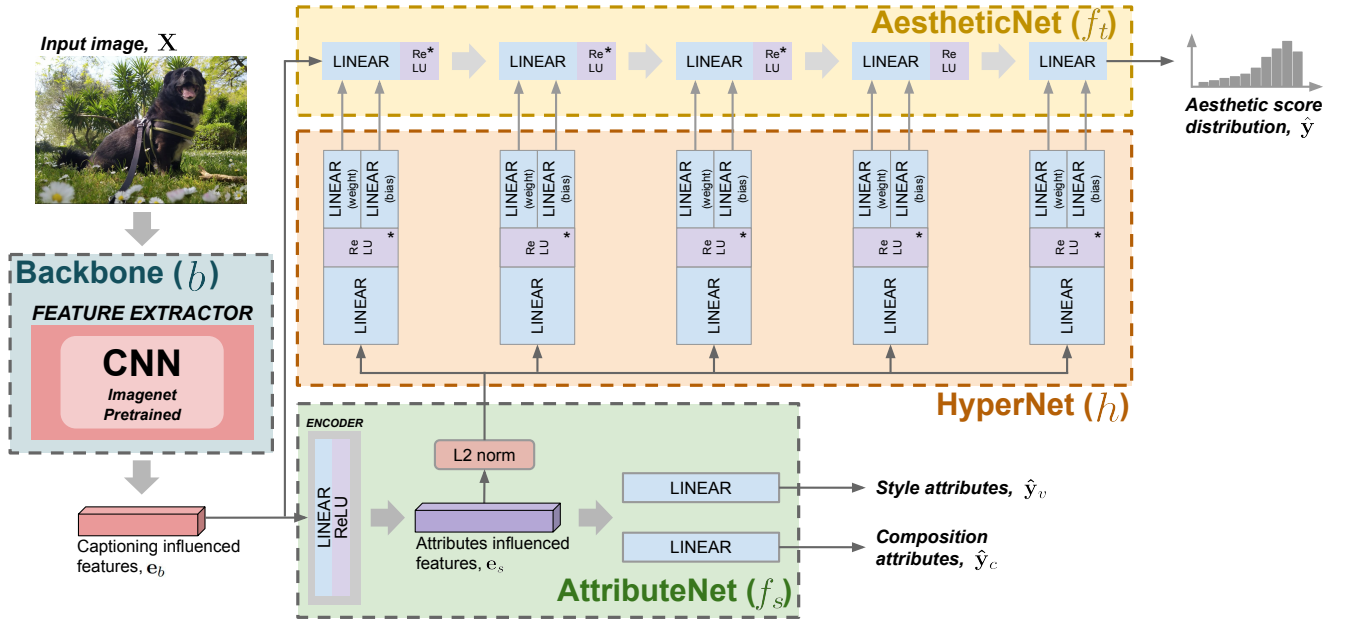


Fig. 2. The proposed method is composed of four main parts: the Backbone (b), the AttributeNet (f_s), the HyperNet (h) and the AestheticNet (f_t). The input image X is first fed to the Backbone to extract a feature set (e_b) that encodes the content of the image. Then, this feature set is fed to AttributeNet. The goal of the AttributeNet is to predict aesthetics-related attributes (i.e. \hat{y}_v and \hat{y}_c) and influence the input of the HyperNet. The HyperNet aims to predict the weights and the biases of the AestheticNet. Finally, the AestheticNet infers the aesthetic score distribution, \hat{y} , of the input image over the content related feature set with the weights and the biases predicted by the HyperNet. *Trained with dropout

C. AestheticNet

The AestheticNet $f_t(e_b; \hat{\theta}_t)$ aims to predict the aesthetic score distribution \hat{q} given the embedding vector e_b produced by the Backbone. It is a MLP composed of M linear layers whose parameters $\hat{\theta}_t = \{(\hat{\mathbf{W}}_1, \hat{\mathbf{b}}_1), (\hat{\mathbf{W}}_2, \hat{\mathbf{b}}_2), \dots, (\hat{\mathbf{W}}_M, \hat{\mathbf{b}}_M)\}$ are computed by the HyperNet h :

$$\mathbf{x}_1 = \text{ReLU}(\hat{\mathbf{W}}_1^\top \mathbf{e}_b + \hat{\mathbf{b}}_1), \quad (7)$$

$$\mathbf{x}_i = \text{ReLU}(\hat{\mathbf{W}}_i^\top \mathbf{x}_{i-1} + \hat{\mathbf{b}}_i), \quad \text{with } i = 2, \dots, M-1 \quad (8)$$

$$\hat{q} = \hat{\mathbf{W}}_M^\top \mathbf{x}_{M-1} + \hat{\mathbf{b}}_M. \quad (9)$$

Since the output of a linear layer is of the same size of the input, thus in correspondence of the following input $\mathbf{x}_{in} \in \mathbb{R}^{N_{in}}$ we have the following output $\mathbf{x}_{out} \in \mathbb{R}^{N_{out}}$. As a consequence, the weights of the layer corresponds to $\mathbf{W} \in \mathbb{R}^{N_{in} \times N_{out}}$ and the bias are equal to $\mathbf{b} \in \mathbb{R}^{N_{out}}$. The number of parameters in a linear layer is $N_{in}N_{out}$ for \mathbf{w} and N_{out} for \mathbf{b} .

D. HyperNet

The HyperNet $h(\mathbf{e}_s; \theta_h^*)$ is the metamodel that generates the parameters θ_t for the M layers of the AestheticNet. Therefore, the HyperNet is composed of M HyperNet Blocks (HBs), $h = \{HB_1, HB_2, \dots, HB_M\}$.

Each HB is composed of a linear layer that reduces the size of the l_2 -normalized embedding $\mathbf{e}_s \in \mathbb{R}^D$ to a size of $d \mid d \ll D$:

$$\mathbf{e}_r = \text{ReLU}(\mathbf{W}_i^{r\top} \mathbf{e}_s + \mathbf{b}_i^r), \quad (10)$$

where ReLU is the activation function, $\mathbf{W}_i^r \in \mathbb{R}^{D \times d}$ are the learned weights, and $\mathbf{b}_i^r \in \mathbb{R}^d$ are the learned bias. Two linear

layers are then dedicated to the estimation of the parameters, \mathbf{W}_i and \mathbf{b}_i of the i -th layer of the AestheticNet:

$$\hat{\mathbf{W}}_i = \mathbf{W}_i^{w\top} \mathbf{e}_r + \mathbf{b}_i^w, \quad (11)$$

$$\hat{\mathbf{b}}_i = \mathbf{W}_i^{b\top} \mathbf{e}_r + \mathbf{b}_i^b. \quad (12)$$

Given the generated weights $\hat{\mathbf{W}}_i \in \mathbb{R}^{N_{in} \times N_{out}}$, the learned parameters of the linear layer are $\mathbf{W}_i^w \in \mathbb{R}^{d \times N_{in}N_{out}}$ and $\mathbf{b}_i^w \in \mathbb{R}^{N_{in}N_{out}}$, respectively. Instead, for the generated bias $\hat{\mathbf{b}}_i \in \mathbb{R}^{N_{out}}$, the learned parameters of the linear layer are $\mathbf{W}_i^b \in \mathbb{R}^{d \times N_{out}}$ and $\mathbf{b}_i^b \in \mathbb{R}^{N_{out}}$.

V. DATASETS

A. Datasets for aesthetic-related attribute recognition

Most previous methods that exploit the relationship between attributes and aesthetic quality rely on the use of the aesthetic attributes provided for the AVA and AADB datasets [17], [32]. Although the two sets of attributes are valuable as they span the traditional photographic principles of color, lighting, focus, and composition, they have some drawbacks. First, they are not exchangeable or can be merged because their annotation are different: in the AVA dataset, annotations are binary values that indicate the occurrence of the attribute in the image; for AADB, the annotation of each attribute can assume continuous values between -1 and 1, where “positive” and “negative” indicates that the occurrence of the attribute improves or degrades the aesthetic level of the image, respectively. Second, only a subset of the AVA images (about 4.44%) provides the style annotations. Third, the number of attributes in the two sets is limited. Few attributes categorize images for composition style (e.g., Rule of Thirds and symmetry). Although the role of

emotion in the aesthetic experience is proven [40], no attributes are specifying what emotions the image content conveys.

Based on the above considerations, and experimental results (see Section VII-D2), the set of aesthetic attributes provided by AADB and AVA is not exploited for the training of the proposed method. Instead, a different and broader set of attributes is considered in this work. Attributes were chosen by taking into account not only the composition but also the style of an image. Among these, there are the optical techniques used during the shot (such as bokeh effect and depth-of-Field), the genre of the image content (e.g., horror or romantic), the atmospheric light conditions (such as hazy or sunny), finally, the mood aroused by the image (e.g., serene).

In this paper we use the KU-PCP [41] and FlickrStyle [42] dataset. The set \mathcal{D}_t is used to train the AttributeNet and it is composed by the two datasets mentioned above. Table I compares the lists of attributes present in the AADB, the AVA datasets and the list of the 29 attributes taken from the KU-PCP and FlickrStyle datasets. We highlight that the set of selected attributes is twice as large as those of AADB (11 attributes) and AVA (14 attributes). Most of the attributes present in the previous sets are also available in the proposed list. We lack attributes such as silhouettes, negative photo, or light on white which are more related to the type of content and not to style or composition.

FlickrStyle: The FlickrStyle dataset [42] is a collection of 80,000 photographs gathered from the Flickr website annotated with 20 curated style labels. These can be categorized into:

- *Atmosphere:* Hazy, Sunny
- *Color:* Bright, Pastel
- *Composition styles:* Detailed, Geometric, Minimal, Texture
- *Genre:* Horror, Noir, Romantic, Vintage
- *Mood:* Ethereal, Melancholy, Serene
- *Optical techniques:* Bokeh, Depth-of-Field, HDR, Long Exposure, Macro

The dataset is split into 64,000 training images and 16,000 testing images. At the time of writing, a total of 63,493 is still downloadable. Thus, the new splits result in 50,868 training images and 12,625 testing images. Images sampled from the dataset are shown in Figure 3a. The FlickrStyle classes are mutually exclusive, that is an image can not have the label “Bright” and the label “Romantic” at the same time.

KU-PCP: The KU-PCP dataset [41] consists of 4,244 outdoor photographs (3,169 for training and 1,075 for testing). It has been annotated by 18 human subject to categorize images into nine not mutually exclusive geometric classes: center, curved, diagonal, horizontal, pattern, Rule of Thirds (RoT), symmetric, triangle, and vertical. Sample images for each category are reported in Figure 3b. The KU-PCP classes are not mutually exclusive, that is an image may have the labels “Rule of Thirds” and “Curved” at the same time.

B. Datasets for image aesthetic assessment

AADB: The Aesthetics and Attributes DataBase (AADB) dataset [11] contains a set of 10,000 images downloaded from

TABLE I
IMAGE ATTRIBUTES AVAILABLE FOR AADB, AVA, AND IN OUR SELECTION.

Attribute Name	AADB [41]	AVA	FlickrStyle + KU-PCP
Balancing elements	✓		
Bright			✓
Bokeh			✓
Center			✓
Color harmony	✓		
Complementary		✓	
Content	✓		
Curved			✓
Depth-of-Field	✓	✓	✓
Detailed			✓
Diagonal			✓
Duotones		✓	
Ethereal			✓
Geometric			✓
Hazy			✓
HDR		✓	✓
Horizontal			✓
Horror			✓
Light	✓		
Light on White		✓	
Long Exposure		✓	✓
Macro		✓	✓
Melancholy			✓
Minimal			✓
Motion Blur	✓	✓	
Negative Photo		✓	
Noir			✓
Object	✓		
Pastel			✓
Photo Grain		✓	
Pattern/Repetition	✓		✓
Romantic			✓
Rule of Thirds	✓	✓	✓
Serene			✓
Silhouettes		✓	
Soft Focus		✓	
Sunny			✓
Symmetry	✓		✓
Texture			✓
Triangle			✓
Vanishing Point		✓	
Vertical			✓
Vintage			✓
Vivid Color	✓		

the Flickr website.¹ Five Amazon Mechanical Turk (AMT) workers annotate each image with an overall aesthetic score and a set of eleven meaningful attributes. These attributes span traditional photographic principals of color, lighting, focus and composition, and are the following: interesting content, object emphasis, good lighting, color harmony, vivid color, shallow depth-of-field, motion blur, Rule of Thirds, balancing element, repetition, and symmetry. For the aesthetic score, AMT workers were allowed to express their judgement on a scale from 1 to 5. For each image, the aesthetic score is the average over all the users judgements. The AADB database was split by its authors into 8,500 images for training, 500 images for validation and 1,000 images for testing. Figure 4a shows the distribution of mean ratings for training and test sets.

AVA: The Aesthetics Visual Analysis (AVA) dataset [24]

¹<http://www.flickr.com>

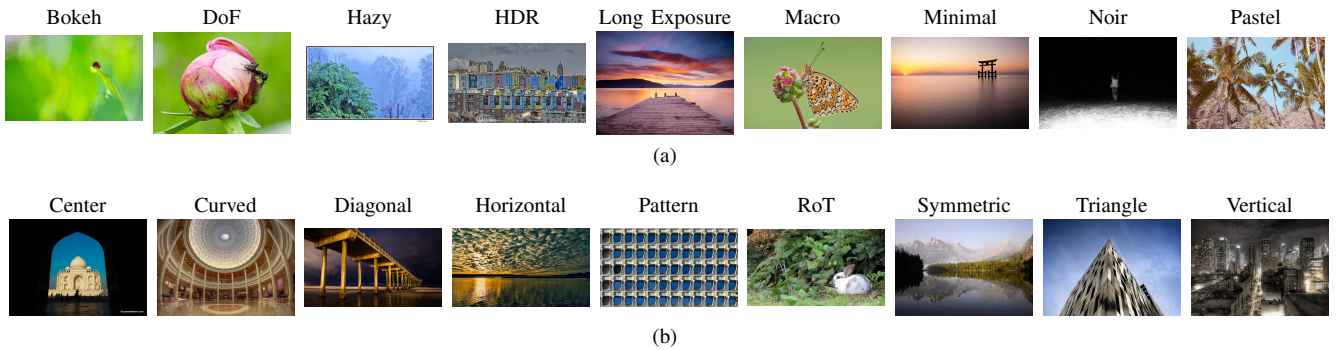


Fig. 3. Sample images from (a) the style categories of the FlickrStyle database [42] and (b) the geometric composition categories of the KU-PCP database [41].

is a large-scale and challenging dataset for image aesthetic assessment. It contains more than 250,000 photos gathered from www.dpchallenge.com. Each image provides three types of annotations: aesthetic ratings ranging from 1 to 10 given by about 200 voters; 0, 1 or 2 textual tags chosen from 66 that describe the semantic content of the image; photographic style annotations corresponding to 14 photographic techniques. From the overall set of images, the authors sampled 20,000 for testing (of which only 19,926 are currently available). Following [16], the remaining 235,574 images are further randomly split into training (95%) and validation (5%) sets. Figure 4b shows the distribution of mean ratings for training and test sets.

Photo.net: The Photo.net dataset [10] is collected from www.photo.net.² It contains 20,278 images annotated by at least 10 users to assess the aesthetic quality from one to seven. Of all the images in the dataset, only 16,662 have the distribution of aesthetics ratings and are available. Following [20], from the overall images, 1000 images are used for validation, 1200 images are used for test, and the remaining 14,462 images are used to train. Since the image indexes for each split are not available from [20], we randomly divide the images based on the previous partitioning. To mitigate any bias due to the data division, we repeat the partitioning 10 times and report the average performance across the 10 runs.

VI. EXPERIMENTS

In this section, we detail the evaluation metrics used to estimate the performance and the training procedure of the proposed method.

A. Evaluation Metrics

We evaluate the proposed method with respect to three aesthetic quality tasks (i) aesthetic score regression, (ii) aesthetic quality classification, and (iii) aesthetic score distribution prediction. For the aesthetic score regression task, we estimate the mean score of the predicted score distribution via $\mu = \sum_{i=1}^N s_i \times p_i$, with s_i representing the score bucket and p_i that is the estimated probability for the i -th bucket. Following [13], [14], [30], for the aesthetic quality classification, we threshold the mean score using the threshold T such that images with

predicted score above T are categorized as high quality and vice versa. The evaluation metrics related to the three task are the following:

- 1) For the image aesthetic score regression, we report results in terms of:
 - SROCC - Spearman’s Rank-Order Correlation Coefficient: this measures the monotonic relationship between the ground-truth and the predicted scores. It ranges from -1 to 1;
 - PLCC - Pearson’s Linear Correlation Coefficient: PLCC measures the linear correlation between the actual and the predicted scores. It ranges from -1 to 1;
 - RMSE - Root Mean Squared Error (RMSE) and MAE - Mean Absolute Error (MAE): these metrics range from 0 to $+\infty$ and smaller values indicate better results.
- 2) For the image aesthetic quality classification, we measure classification performance in terms of the overall accuracy, defined as $Accuracy = \frac{TP+TN}{P+N}$.
- 3) For the image aesthetic score distribution prediction, we use Earth Mover’s Distance (EMD) to estimate the closeness of the predicted and ground-truth rating distributions. The EMD is defined in Equation 15 with $r = 1$ and lower values of EMD mean better results.

B. Training Procedure

The learnable parameters of the proposed model are exclusively θ_s and θ_h , i.e. those of the AttributeNet f_s and those of the HyperNet h . In fact, as previously described in Section IV, the θ_b^* parameters belong to a fixed ImageNet-trained Backbone. On the other end, the AestheticNet receives the generated parameters $\hat{\theta}_i$ from the HyperNet.

Similar to [35], we adopt a two-step optimization procedure to introduce attribute-constraint into the HyperNet. We first train the AttributeNet for aesthetic-related attributes recognition. We then freeze the AttributeNet and train the HyperNet for the aesthetic assessment.

Both the AttributeNet and the AestheticNet receive the embedding e_b produced by the pre-trained Backbone as input. To reduce the training time, as in [16] and [23], we store the embedding produced by the Backbone for the dataset images instead of calculating them at each training process.

²Available at <http://ritendra.weebly.com/aesthetics-datasets.html>

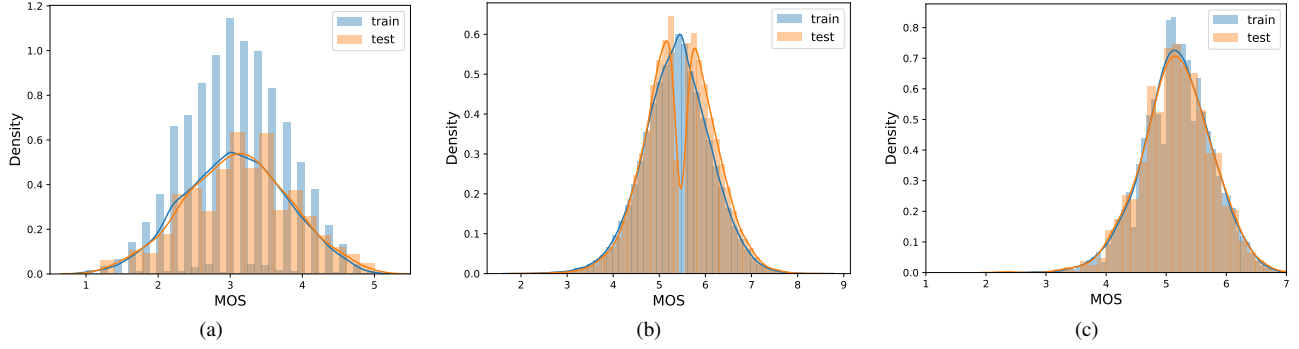


Fig. 4. Distributions of the aesthetic scores on the AADB [11] (a), AVA [24] (b), and Photo.net [10] (c) datasets.

a) Training for aesthetic-related attributes recognition:

We exploit Multi-Task Learning (MTL) to train the Multi Layer Perceptron parameters θ_s of the AttributeNet for predicting both image style and image composition. Let $\theta_s = \{\mathbf{W}_s, \mathbf{W}_v, \mathbf{W}_c\}$ represent the weights for the AttributeNet. The bias terms are eliminated for simplicity. Given the dataset $\mathcal{D}_v = \{(\mathbf{X}_v^{(i)}, \mathbf{y}_v^{(i)})\}_{i=1}^M$ for image style recognition and the dataset $\mathcal{D}_c = \{(\mathbf{X}_c^{(i)}, \mathbf{y}_c^{(i)})\}_{i=1}^N$ for image composition recognition, our AttributeNet aims to minimize the combined loss of both tasks:

$$\operatorname{argmin}_{\theta_s} a_v \sum_{i=1}^M \mathcal{L}_v(\mathbf{e}_b^{(i)}, \mathbf{y}_v^{(i)}) + a_c \sum_{j=1}^N \mathcal{L}_c(\mathbf{e}_b^{(j)}, \mathbf{y}_c^{(j)}), \quad (13)$$

where a_v and a_c control the importance of each task and correspond to 1 and 10, respectively (see Sec. VII-D3 for the analysis of these two hyperparameters). The embedding $\mathbf{e}_b^{(i)} = b(\mathbf{X}_v^{(i)}; \theta_b^{*(L)})$, $\mathbf{e}_b^{(j)} = b(\mathbf{X}_c^{(j)}; \theta_b^{*(L)})$ are obtained from the Backbone for both the training sets.

The dataset \mathcal{D}_v used for style recognition is FlickrStyle. As described in Section V, the twenty FlickrStyle categories have been annotated as mutually exclusive therefore we adopt cross-entropy as \mathcal{L}_v . The KU-PCP dataset instead is adopted as \mathcal{D}_c . KU-PCP is labeled with nine not mutually exclusive image composition classes. Hence, we use the binary cross-entropy as the \mathcal{L}_c loss function. The cardinality of the image style recognition dataset is greater than that of the image composition: the FlickrStyle dataset has 50,868 training images, while KU-PCP consists of 3,169 training images. For this reason, during the training phase, we balance the number of images between the two datasets by performing data augmentation on KU-PCP. We select augmentation techniques that do not affect the image composition, i.e., color jittering (random adjustment of brightness, contrast, saturation, hue), random horizontal flipping, random grayscale, and random patch erasing.

The size of the embedding vector \mathbf{e}_s is fixed to 512. The learning rate is initially set to $1e^{-4}$ and then dropped by 10 every 20 epochs. We use a batch size of 32, randomly sampling images from both the KU-PCP and the FlickrStyle. We train the model for a maximum of 60 epochs using Adam [43] as optimizer monitoring the accuracy over the validation set to select the best model.

b) Training for aesthetic assessment: The second training concerns the θ_h parameters of the HyperNet for generating

the parameters $\hat{\theta}_t$ of the AestheticNet, which in turn manages the aesthetic assessment. In this paper, we formulate the aesthetic assessment as a label distribution prediction problem. More in detail, our network f_t is not trained to predict the Mean Opinion Score (MOS), instead it infers the l_1 -normalized score distribution $\hat{\mathbf{q}} = [\hat{q}_{s_1}, \hat{q}_{s_2}, \dots, \hat{q}_{s_B}]$. Where s_i is the i -th score bucket, B is the total number of score buckets, and \hat{q}_{s_i} denotes the number of voters that give the discrete score s_i to the image.

Given the dataset $\mathcal{D}_t = \{(\mathbf{X}_t^{(k)}, \mathbf{q}^{(k)})\}_{k=1}^N$, the ground-truth of each image k is represented by a score distribution $\mathbf{q} = [q_{s_1}, q_{s_2}, \dots, q_{s_B}]$ defined as above. We optimize the HyperNet as follows:

$$\operatorname{argmin}_{\theta_h} \sum_{k=1}^N \mathcal{L}_{task}(\mathbf{e}_s^{(k)}, \mathbf{q}^{(k)}), \quad (14)$$

where $\mathbf{e}_s^{(k)} = f_s(\mathbf{e}_b; \theta_s^{*(M)})$ is the attribute-conditioned embedding obtained from the previously trained AttributeNet for the training image $\mathbf{X}_t^{(k)}$. The loss \mathcal{L}_{task} is the Earth Mover's Distance (EMD). Given the predicted $\hat{\mathbf{q}}$ and the ground-truth \mathbf{q} score distributions, the EMD loss function is defined as follows:

$$\operatorname{EMD}(\hat{\mathbf{q}}, \mathbf{q}) = \left(\frac{1}{N} \sum_{k=1}^N |CDF_{\hat{\mathbf{q}}}(k) - CDF_{\mathbf{q}}(k)|^r \right)^{\frac{1}{r}}, \quad (15)$$

where $CDF_*(k)$ is the cumulative distribution function, r equal to 2 is used to penalize the Euclidean distance between the CDFs.

The AestheticNet consists of $M = 5$ linear layers whose output sizes are 512, 256, 256, 64, respectively. The last linear layer have a number of neurons in output equal to the number of buckets of the score distribution which depends on the training dataset: AADB dataset have a total of 5 buckets ($B = 5$) with $s_1 = 1$ and $s_B = 5$; AVA dataset have a total of 10 buckets ($B = 10$) with $s_1 = 1$ and $s_B = 10$; the Photo.net dataset, $B = 7$, $s_1 = 1$, $s_B = 7$. We run this training for 40 epochs exploiting the Adam optimizer. The initial learning rate corresponds to $1e^{-5}$, then it is divided by 10 every 20 epochs. We track the SROCC over the validation set to select the best model.

VII. RESULTS

In this section, we first report the results obtained by the method proposed for aesthetic-related attribute recognition. We then measure the effectiveness of the proposed method for image aesthetic assessment on the three considered datasets, namely AADB, AVA, and Photo.net. Next, we compare our results with those of many other methods in the state-of-the-art. Finally, we perform an ablation study on the AVA dataset.

Figure 5 shows some predictions produced by the proposed method on the AVA test images. For each image, we report the mean score of the aesthetic distribution and the style and composition tags predicted by our method, as well as the corresponding ground-truths. As can be seen, the proposed method provides an aesthetic quality estimate in close agreement with human judgments. The predictions for composition and style attributes almost coincide with those provided by ground-truth, and even those for which a ground-truth is not available (N/A: absent style or composition information), the prediction is plausible.

A. Image style and composition recognition

We evaluate the performance of our method for the image style recognition task on the FlickrStyle dataset and for the image composition recognition on the KU-PCP dataset.

We achieve 0.462 of average precision on the 12,625 test images of the FlickrStyle dataset. On the other hand, the method proposed by Karayev *et al.* [42] achieves 0.368 of average precision on the FlickrStyle test set. Moreover, the average precision in [42] is estimated on a random subset of the test data balanced so that each class has equal cardinality. Figure 6 reports the confusion matrix on the 20 style categories. We highlight that our model performs well on styles like Macro (77.20% of accuracy), Noir (66.48%), and Sunny (62.75%) while it is less effective on styles like Romantic (19.93%) and Depth-of-Field (17.36%). The worst misclassification cases concern the following couples: Depth-of-Field vs. Bokeh; Horror vs. Noir; Pastel vs. Vintage.

We evaluate the performance of our method for image composition recognition on the test set of the KU-PCP dataset. We measure the accuracy score in terms of $accuracy = \frac{N_c}{N}$ where N and N_c are the numbers of the total and correctly classified photographs, respectively. Following [41], we consider an image correctly classified if it is assigned to at least one of the ground-truth composition classes. Our model registers an accuracy of 70.87% which is in line with the performance of the authors training an SVM classifier over the deep features extracted from a CNN pre-trained on ImageNet, which achieve an accuracy of 70.23%. In Figure 7 we show the confusion matrix on the 9 categories of KU-PCP.

B. Image aesthetic assessment

In this section, we present the results obtained by the proposed method for the image aesthetic assessment. For each of the three benchmark datasets, namely AADB, AVA, and Photo.net, we measure performance in terms of Accuracy, Spearman’s Rank-Order Correlation Coefficient (SROCC),

Pearson’s Linear Correlation Coefficient (PLCC), Mean Absolute Error (MAE), Root Mean Squared Error (RMSE), and Earth Mover’s Distance (EMD).

We compare ours with several state-of-the-art methods. For these methods, we quote the performance declared in the original papers. In addition to the results of the different methods, we calculate a baseline (named as “Baseline”) by considering a dummy solution that assigns the average of the training set scores to each test image. More specifically, for each test image, we generate a normal distribution with a mean equal to the mean of the training set scores and a randomly sampled standard deviation in the interval $[-0.5, 0.5]$.

Table II reports the results on the AADB dataset. From the results it is possible to draw several conclusions. First, the proposed method outperforms all state-of-the-art methods for the SROCC metric which is the only one to be reported by all methods. Second, our method outperforms Leonardi *et al.* [23] for all metrics. In particular, our accuracy is 2% higher than that of the Leonardi. Finally, the third method, i.e. *RGNet* [4], has a SROCC of 0.03 lower than the proposed method.

In Table III the results on the AVA dataset are reported. The *Baseline* obtained a precision of 71.28% which is 12% lower than the best precision corresponding to 83.59% for *RGNet* and only 3% lower than the method with the worst accuracy, namely *RAPID*. This indicates that methods having a good fit with the training score distribution tend to perform well on test data since the two distributions are very similar (see Fig. 4b for details). Interestingly, no method achieves the best performance for all metrics. *RGNet* obtains the best accuracy, while MLSP [16] shows the highest regression metrics against mid-ranking accuracy (81.68%). The proposed method ranks second for the regression metrics, first for the EMD metric, while it achieves an accuracy 3% lower than the 83.59% by *RGNet*.

Figure 8 shows ten samples from the AVA test set predicted by the proposed method as having high aesthetic quality (the top five images) and low aesthetic quality (the bottom five images), respectively. Plots of the ground-truth and predicted distributions are also shown. As it is possible to see, the model can achieve a high degree of accuracy, with an estimate of the score distribution almost perfect in some cases. In Figure 9 there are two examples of failure of our method on the AVA test set images. The method behaves badly on images with not very Gaussian score distributions. This might depend on the fact that 99.77% of the images in the dataset instead follows a Gaussian distribution [24].

Finally, Table IV shows the comparison on the Photo.net dataset. The results for state-of-the-art methods are reported by [20]. We underline that the performance is not directly comparable. The evaluation protocols adopted for the methods are different (see the column “Evaluation protocol” for details about the adopted protocols). Our performance is comparable to that reported for *GPF-CNN* that is the method achieving results similar to ours.

Several things can be deduced from the results. First, the *Baseline* accuracy is very high (66.58%) compared to the average obtained by the methods on this dataset. It exceeds that of three methods, i.e. *GIST_SVM* [22], *FV_SIFT_SVM*



Fig. 5. Output produced by the proposed method on sample images from the AVA dataset. For each image, the aesthetic score and the attributes predicted by the proposed method are reported (ground-truth is in brackets). “N/A” means that the dataset does not provide any style annotation for the image.

TABLE II

COMPARISON OF THE PROPOSED METHOD WITH STATE-OF-THE-ART METHODS ON THE AADB DATASET. THE “-” MEANS THAT THE RESULT IS NOT AVAILABLE. THE NETWORK ARCHITECTURE AND WHETHER IT USES MULTI-TASK LEARNING (MTL) IS INDICATED FOR EACH METHOD.

Method	Network architecture	MTL	Accuracy (%) \uparrow	SROCC \uparrow	PLCC \uparrow	MAE \downarrow	RMSE \downarrow	EMD \downarrow
Baseline			61.58	-0.0744	-0.0543	0.1449	0.1799	0.1407
Reg-Net [11]	AlexNet		-	0.6782	-	-	-	-
Malu <i>et al.</i> [44]	ResNet-50	\checkmark	-	0.6890	-	-	-	-
PI-DCNN [17]	ResNet-50	\checkmark	-	0.7051	-	-	-	-
Chen <i>et al.</i> [45]	ResNet-50		-	0.7080	-	-	-	-
Pan <i>et al.</i> [18]	ResNet-50	\checkmark	-	0.7041	-	-	-	-
Reddy <i>et al.</i> [38]	EfficientNet-B4	\checkmark	-	0.7059	-	-	-	-
RGNet [4]	DenseNet-121		-	0.7104	-	-	-	-
Leonardi <i>et al.</i> [23]	EfficientNet-B4		79.51	0.7454	0.7479	0.1062	0.1351	-
Proposed	EfficientNet-B4	\checkmark	81.64	0.7567	0.7616	0.0832	0.1059	0.0951

TABLE III

COMPARISON OF THE PROPOSED METHOD WITH STATE-OF-THE-ART METHODS ON THE AVA DATASET. IN EACH COLUMN, THE BEST AND SECOND-BEST RESULTS ARE MARKED IN **BOLDFACE** AND UNDERLINED, RESPECTIVELY. THE “-” MEANS THAT THE RESULT IS NOT AVAILABLE. THE NETWORK ARCHITECTURE AND WHETHER IT USES MULTI-TASK LEARNING (MTL) IS INDICATED FOR EACH METHOD.

Method	Network architecture	MTL	Accuracy (%) \uparrow	SROCC \uparrow	PLCC \uparrow	MAE \downarrow	RMSE \downarrow	EMD \downarrow
Baseline			71.28	-0.0003	-0.0021	0.6230	0.7550	0.0743
RAPID [12]	AlexNet		74.20	-	-	-	-	-
DMA-Net [29]	AlexNet		75.42	-	-	-	-	-
MNA-CNN [30]	VGG16		76.10	-	-	-	-	-
Reg-Net [11]	AlexNet		77.33	0.5581	-	-	-	-
MTCNN [13]	VGG16	\checkmark	78.56	-	-	-	-	-
Multimodal DBM Model [28]	VGG16		78.88	-	-	-	-	-
NIMA [19]	VGG16		80.60	0.5920	0.6100	-	-	0.0520
GPF-CNN [20]	VGG16		80.70	0.6762	0.6868	0.4144	0.5347	0.0460
NIMA [19]	InceptionNet		81.51	0.6120	0.6360	-	-	0.0500
MLSP [16]	InceptionNet		81.68	0.7524	0.7545	0.3831	0.4943	-
GPF-CNN [20]	InceptionNet		81.81	0.6900	0.7042	0.4072	0.5246	0.0450
MULTIGAP [27]	InceptionNet		82.27	-	-	-	-	-
A-Lamp [14]	VGG16		82.50	-	-	-	-	-
AFDC+SPP [21]	ResNet-50		<u>83.24</u>	0.6489	0.6711	-	-	<u>0.0447</u>
PI-DCNN [17]	ResNet-50	\checkmark	-	0.6578	-	-	-	-
Pan <i>et al.</i> [18]	ResNet-50	\checkmark	-	0.7041	-	-	-	-
RGNet [4]	DenseNet-121		83.59	-	-	-	-	-
Proposed	EfficientNet-B4	\checkmark	80.75	<u>0.7318</u>	<u>0.7329</u>	<u>0.4011</u>	<u>0.5128</u>	0.0439

[22], and *MTCNN* [13]. Second, the proposed method records a significant improvement on all metrics apart from accuracy compared to *GPF-CNN*. In particular, the SROCC of 0.5650 is 0.04 higher than that of *GPF-CNN*, the MAE is 0.05 lower. Third, the small standard deviation indicates that the proposed method is able to generalize well.

C. Image aesthetic assessment on specific attributes

In this section, we show how the method works separately for various aesthetic attributes. We select images from the test

set of the AVA dataset for the five attributes that are present in AVA and can be discriminated by our method: i.e. Depth-of-field, HDR, Long Exposure, Macro, and Rule of Thirds. The collection consists of about 150 images for each attribute. In each category of images, we systematically estimate the ability of our classifier, namely AttributeNet, to recognize the dominant attribute and of our AestheticNet to estimate aesthetic quality. The experimental results are illustrated in Table V. These results indicate that the proposed method is able to recognize the attributes even on unseen data, in fact the

TABLE IV

COMPARISON OF THE PROPOSED METHOD WITH STATE-OF-THE-ART METHODS ON THE PHOTO.NET DATASET. IN EACH COLUMN, THE BEST AND SECOND-BEST RESULTS ARE MARKED IN **BOLDFACE** AND UNDERLINED, RESPECTIVELY. THE “-” MEANS THAT THE RESULT IS NOT AVAILABLE. THE NETWORK ARCHITECTURE AND WHETHER IT USES MULTI-TASK LEARNING (MTL) IS INDICATED FOR EACH METHOD.

Method	Net. arch.	MTL	Accuracy (%) \uparrow	SROCC \uparrow	PLCC \uparrow	MAE \downarrow	RMSE \downarrow	EMD \downarrow	Evaluation protocol
Baseline			66.58 \pm 0.30	0.0060 \pm 0.02629	0.0053 \pm 0.0285	0.4481 \pm 0.0023	0.5652 \pm 0.0023	0.0789 \pm 0.0004	15K train, 1000 val, 1200 test*
GIST_SVM [22]			59.90	-	-	-	-	-	5-fold cross-validation
FV_SIFT_SVM [22]			60.80	-	-	-	-	-	5-fold cross-validation
MTCNN [13]	VGG16	\checkmark	65.20	-	-	-	-	-	about 15K train, 3000 test
GPF-CNN [20]	VGG16		75.60	0.5217	0.5464	0.4242	0.5211	0.0700	15K train, 1000 val, 1200 test
Proposed	EfficientNet-B4	\checkmark	<u>70.05 \pm 0.89</u>	0.5650 \pm 0.0153	0.5698 \pm 0.0141	0.3714 \pm 0.0065	0.4700 \pm 0.0071	0.0689 \pm 0.0009	15K train, 1000 val, 1200 test*

* Average and standard deviation on the 10 iterations of train-val-test splits.

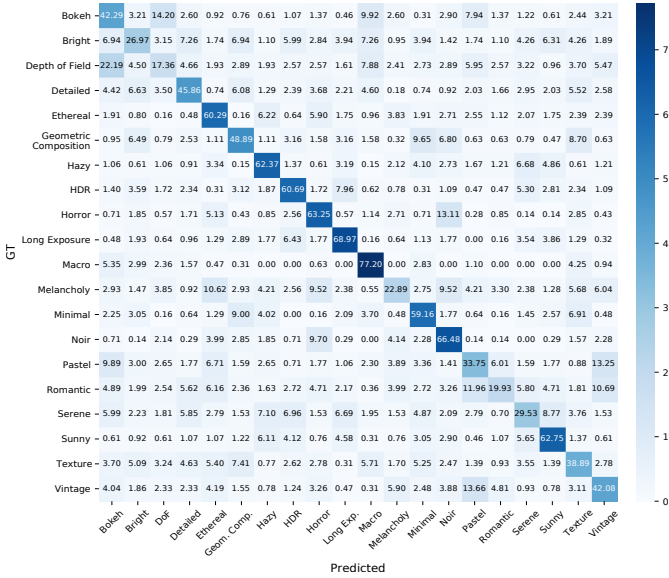


Fig. 6. Confusion matrix on the Flickr Style categories.

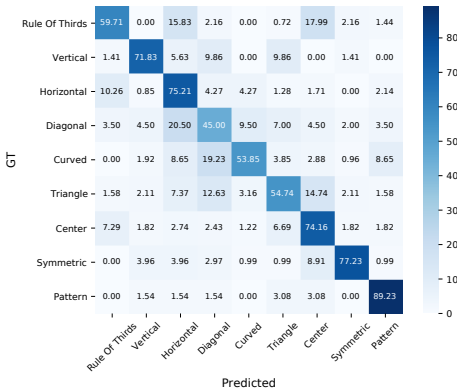


Fig. 7. Confusion matrix for image composition recognition on the KU-PCP test set.

accuracy performance obtained is very similar to that reported for the same classes in the confusion matrix in Figure 6. Macro is easier to recognize with 76.39% accuracy, while Depth-of-Field is more challenging with a percentage equal to 56.46%.

By analyzing the aesthetic performance for the five attributes, we notice that the best performance is attained for all the considered metrics for the images belonging to the category HDR. We can also find that the performance of the proposed method significantly drops for images labeled as

Depth-of-field. This behavior, which may be due to our method failing to categorize images well for that attribute, indicates that our aesthetic assessment process is indeed attribute-driven.

D. Ablation study

1) *Effectiveness of the designed model architecture:* Unlike traditional methods and architectures, the use of an attribute-conditioned hypernetwork in the proposed method allows to have a dedicated aesthetic evaluator for each test image that depends on the composition and style attributes it contains. At the same time the hypernetwork adds an extra compute load to the network to generate the AestheticNet parameters. Here, we present two experiments aimed at justifying the design choices of the proposed architecture. In the first experiment we validate the effectiveness of the hypernetwork. We compare the performance obtained by the proposed method with that of a simplified version of our proposal without hypernetwork. Specifically, we remove the HyperNet, and the embedding of the AttributeNet e_s is mapped to the aesthetic score distribution through a linear layer. We follow the same training procedure presented in Section VI-B for a fair comparison. The second experiment is aimed at demonstrating the importance of guiding the aesthetic prediction by exploiting composition and style attributes. For this purpose, we perform a surgical operation to the proposed method in which we remove AttributeNet and HyperNet. The embedding vector e_b estimated by the Backbone is mapped to an aesthetic score distribution using the AestheticNet’s MLP, whose weights are learned on the aesthetic dataset.

Table VI reports the results of the ablation study on the AVA test images. In the “AttrNet + AesthNet (Linear)” row we show the results for the solution with a linear layer as AestheticNet, while in the “AesthNet (MLP)” there are the results of the Backbone followed by an MLP as AestheticNet. As can be seen, both variants of the method achieve worse results than the proposed method. In detail, the drop obtained by the “AttrNet + AesthNet (Linear)” variant is 2% in terms of accuracy and 0.07 for the SROCC. The fact that the drop obtained by “AesthNet (MLP)” compared to our best solution is even greater (i.e., 3% less for binary classification and 0.08 for both PLCC and SROCC) experimentally supports the choice of having characterized the attributes and the adopted design choices.

2) *Impact of the AttributeNet characterization on the aesthetic assessment:* Since the aesthetic assessment process is

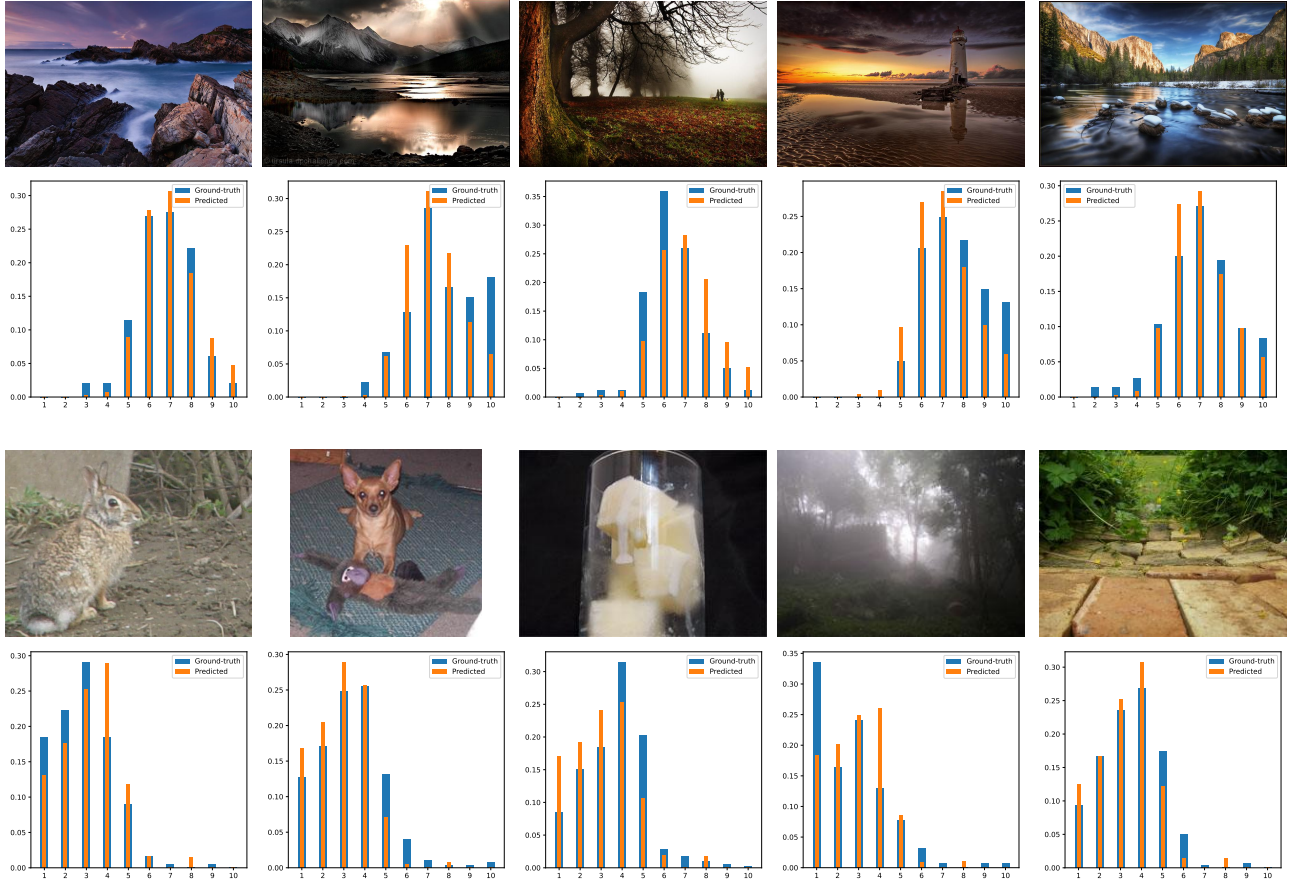


Fig. 8. Sample predictions by our method on AVA test images. Top 2 rows: predicted images with high aesthetic quality, coupled with plots of their ground-truth and predicted score distributions. Bottom 2 rows: predicted images with low aesthetic quality, coupled with plots of their ground-truth and predicted score distributions.

TABLE V
PERFORMANCE ON FIVE AESTHETIC-RELATED ATTRIBUTES OF THE AVA DATASET.

Attribute	Attribute recognition		Aesthetic assessment				
	Acc. (%) \uparrow	Acc. (%) \uparrow	SROCC \uparrow	PLCC \uparrow	MAE \downarrow	RMSE \downarrow	EMD \downarrow
Depth-of-field	56.46	79.31	0.7320	0.7575	0.4129	0.5006	0.0448
HDR	59.52	92.86	0.7944	0.8007	0.3110	0.3902	0.0347
Long Exposure	65.25	81.35	0.6506	0.7741	0.4025	0.4985	0.0435
Macro	76.39	82.32	0.7941	0.7616	0.3528	0.4518	0.0408
Rule of Thirds	64.52	80.29	0.6942	0.6732	0.3757	0.4804	0.0406

TABLE VI
ABLATION STUDY RESULTS ON THE AVA TEST SET. EACH ROW REPORTS THE RESULTS FOR A MODIFIED VERSION OF THE PROPOSED METHOD. THE BACKBONE IS PRESENT IN ALL VARIANTS BUT IS OMITTED FOR SIMPLICITY.

Method	Acc. (%) \uparrow	SROCC \uparrow	PLCC \uparrow	MAE \downarrow	RMSE \downarrow	EMD \downarrow
AttrNet + AesthNet (Linear)	78.59	0.6600	0.6633	0.4420	0.5652	0.0481
AesthNet (MLP)	77.65	0.6546	0.6559	0.4529	0.5875	0.0496
AttrNet (only style) + HyperNet + AesthNet	79.78	0.7269	0.7302	0.4115	0.5243	0.0475
AttrNet (only comp.) + HyperNet + AesthNet	80.23	0.7295	0.7312	0.4092	0.5197	0.0461
AttrNet (on AVA) + HyperNet + AesthNet	78.76	0.6676	0.6714	0.4360	0.5595	0.0485
AttrNet + HyperNet + AesthNet	80.75	0.7318	0.7329	0.4011	0.5128	0.0439

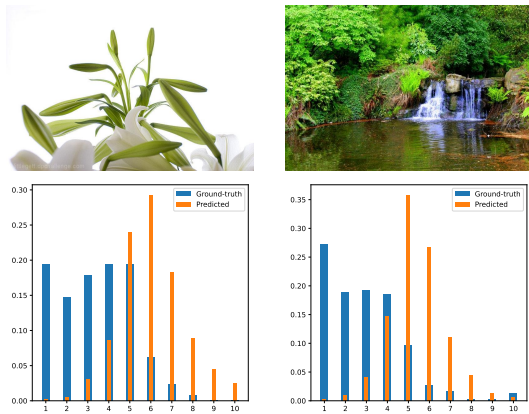


Fig. 9. Failure cases of our method on the AVA test set images.

guided by the characterized attributes, the effectiveness of the proposed method also depends on the goodness of the representation obtained from AttributeNet and consequently on the concepts on which it is trained. In this section we comprehensively measure the effect on aesthetic evaluation determined by the data used to train the AttributeNet.

The first set of experiments consists of training AttributeNet to discriminate only the style or composition of the image. In the first experiment, we run the first training of our method for aesthetic-related attributes recognition to discriminate the 20 photographic styles of the FlickrStyle dataset. The training for aesthetic assessment, which affects only the HyperNet, exploits the weights learned on FlickrStyle of the AttributeNet. The results for this solution are reported in the row “AttrNet (only style) + HyperNet + AesthNet” of Table VI. Differently from the previous experiment, in the second experiment the training of the AttributeNet learns how to estimate the compositional rules of the KU-PCP. In the row “AttrNet (only comp.) + HyperNet + AesthNet” of Table VI, we show the results for this experiment. We can see how the results obtained for both experiments are worse than those obtained by training AttributeNet for simultaneous estimation of style and composition. Furthermore, the version in which the AttributeNet is trained for discriminating the image composition works better than the one in which the photographic styles are estimated. This latter result indicates that somehow composition has a greater importance than styles in estimating image aesthetics.

In another experiment, we evaluate the effectiveness of using only AVA’s photographic styles to train the AttributeNet. This experiment serves to quantitatively evaluate the outcome due to the use of additional data to characterize the aesthetic-related attributes. Of the 250,000 images in the AVA dataset, we use the 14,079 images labeled with one of the 14 photographic styles to training AttributeNet (see Table I for details on what those styles are). The training for aesthetic assessment is then carried out by exploiting the AttributeNet trained on AVA styles and without the use of additional data. As can be seen from the results in the row “AttrNet (on AVA) + HyperNet + AesthNet” of the Table VI, the performance obtained in this experiment is significantly lower than that of our final solution. The reason for this drop is due to the fact that AVA provides

labels for the photographic style and no attributes regarding the composition. We have seen in previous experiments that the composition helps the aesthetic estimation with respect to the photographic style. Certainly the main cause of this poor result is that a few data is available for AttributeNet training as few AVA images are annotated with the style.

A qualitative comparison of the variants of the proposed method evaluated in the ablation study is shown in Figure 10.

3) *AttributeNet hyperparameter tuning*: In this subsection we study the effect of the two parameters a_v and a_c defined in Equation 13 for AttributeNet training. Since two different datasets are used for training, the choice of these parameters can affect the stability of the training. To this end, the training procedure presented in Section VI-B for aesthetics-related attributes recognition is carried out by varying the value of the previous parameters. Figure 11 shows the average accuracy for the two tasks by varying the parameter values. It is possible to notice how as the value of a_v decreases and the value of a_c increases, the accuracy on the two tasks increases until it reaches the highest value of 61.67% for $a_v = 1$ and $a_c = 10$, respectively.

E. Visualization of predicted weights

To assess the influence of the style of the images over the aesthetics prediction, we extract the weights $\hat{\theta}_t$ generated by the HyperNet from several images of the AVA test set.

We annotate all 12,625 test images of the FlickrStyle dataset with the proposed method. We randomly select 200 images for each of the 20 style categories and store the weights \bar{W}_5 of the last AestheticNet linear layer generated by the HyperNet. We then reduce the size of the predicted weights with t-distributed Stochastic Neighbor Embedding (t-SNE) [46] and plot them in a 2D space for visualization.

Figure 12 shows the projection of each selected test image in the two-dimensional space. The weights generated for the other levels of the AestheticNet show a similar distribution. Each point has a different color based on the predicted style category. In the three enlargements, we report a few sample images with the aesthetic scores (predicted and the corresponding ground-truth in brackets).

Several interesting behaviors can be observed from the figure. First, for different images, the generated weights are different. This behavior indicates that our method adopts distinct weights to evaluate the aesthetics of the image in a self-adaptive manner. While for traditional models of automatic aesthetic assessment, the weights are fixed for all input images. Second, images belonging to the same image style (e.g. HDR, pastel, macro) generate weights that are close to each other. This verifies that the training of the AttributeNet is effective. Furthermore, it is noticeable how the information encoded in the embedding produced by the AttributeNet is successfully propagated through the whole model.

VIII. CONCLUSION

In this article, we presented a self-adaptive method for image aesthetic assessment. Since the aesthetic evaluation of images is influenced by the content and aesthetic-related

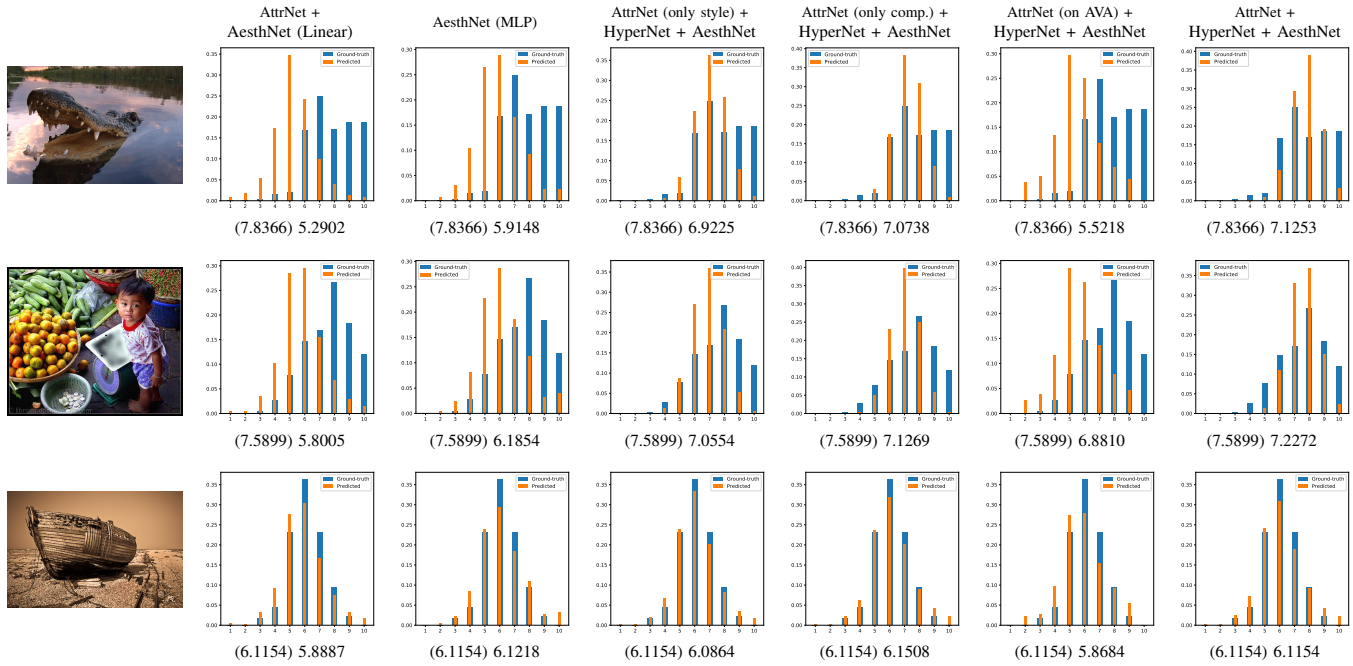


Fig. 10. Qualitative comparison of different versions of the proposed method on three AVA test images. The sampled images are paired with plots of their ground-truth and predicted score distributions. The aesthetic and ground-truth score (in brackets) are also reported under each plot.

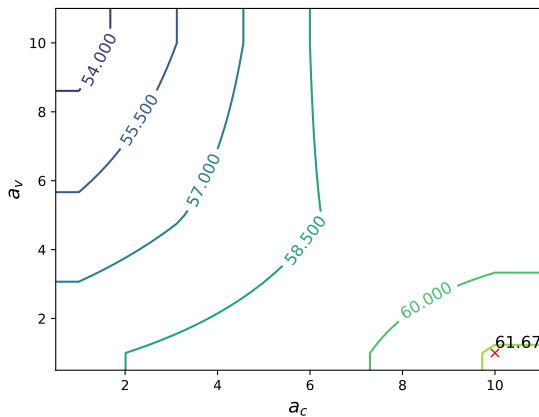


Fig. 11. Average accuracy for the composition and style recognition tasks as the values assumed by the parameters a_c and a_v defined in the Equation 13 vary. The red cross highlights the best configuration that achieves the best accuracy.

attributes, we designed a method that models the aesthetics of the image by explicitly considering semantic content, style, and composition. In particular, the proposed method exploits the side information relating to the aesthetic attributes of an image to build an *ad-hoc* image aesthetics estimator. The parameters of the aesthetic estimator are adaptively generated from a metamodel consisting of an attribute-conditioned hypernetwork. Given an image, the resulting model predicts (i) the style and composition of the image, (ii) the aesthetic score distribution.

Experimental results on three benchmark datasets, namely AADB [11], AVA [24], and Photo.net [10] show that the proposed method achieves comparable performance to previous methods for aesthetic quality classification. Instead, it

outperforms state-of-the-art methods for both image aesthetic score regression and aesthetic score distribution prediction. Ablation experiments show that aesthetic-attributes, in particular composition rules, allow to obtain an aesthetic evaluation correlating better with human judgments. Furthermore, having attribute-specific aesthetic estimators thanks to the use of the hypernetwork results in better effectiveness of the proposed method with respect to state-of-the-art methods.

Regardless of the obtained results, we believe that the approach integrating attribute-related knowledge in the aesthetic evaluation process represents a step towards a deeper understanding of aesthetic clues. Furthermore, it is highly scalable to new data or aesthetic-related tasks.

REFERENCES

- [1] M. Freeman, *The complete guide to light & lighting in digital photography*. Sterling Publishing Company, Inc., 2007.
- [2] P. Shamo, A. Inoue, and H. Kawanaka, “Modeling aesthetic preferences: Color coordination and fuzzy sets,” *Elsevier Fuzzy Sets and Systems*, vol. 395, pp. 217–234, 2020.
- [3] J. Itten, *Design and form: The basic course at the Bauhaus and later*. John Wiley & Sons, 1975.
- [4] D. Liu, R. Puri, N. Kamath, and S. Bhattacharya, “Composition-aware image aesthetics assessment,” in *Winter Conference on Applications of Computer Vision*, 2020, pp. 3569–3578.
- [5] L. Celona and R. Schettini, “A genetic algorithm to combine deep features for the aesthetic assessment of images containing faces,” *MDPI Sensors*, vol. 21, no. 4, p. 1307, 2021.
- [6] W. Luo, X. Wang, and X. Tang, “Content-based photo quality assessment,” in *International Conference on Computer Vision (ICCV)*. IEEE, 2011, pp. 2206–2213.
- [7] P. Obrador, L. Schmidt-Hackenberg, and N. Oliver, “The role of image composition in image aesthetics,” in *International Conference on Image Processing*. IEEE, 2010, pp. 3185–3188.
- [8] Kodak, *How to take good pictures: a photo guide*. Ballantine Books, 1981.
- [9] M. Freeman, *The photographer’s eye: composition and design for better digital photos*. Routledge, 2017.

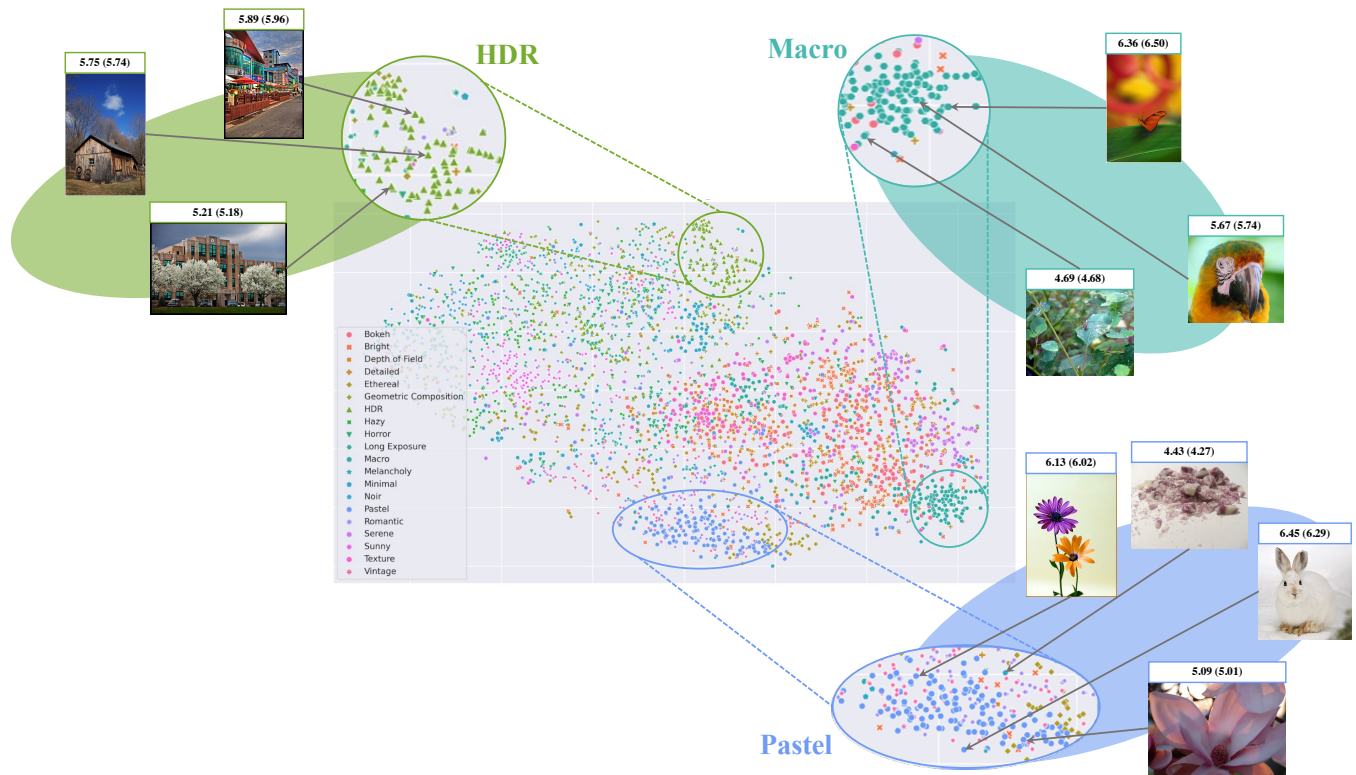


Fig. 12. The predicted weights for several images of the AVA test set are plotted in the 2D space after the t-SNE transformation. This figure shows the weights extracted from the last layer of the target network, the weights of the other layers also show a similar distribution. For each of the depicted images, we report the predicted aesthetic score (ground-truth is in brackets).

[10] R. Datta, D. Joshi, J. Li, and J. Z. Wang, "Studying aesthetics in photographic images using a computational approach," in *European Conference on Computer Vision (ECCV)*. Springer, 2006, pp. 288–301.

[11] S. Kong, X. Shen, Z. Lin, R. Mech, and C. Fowlkes, "Photo aesthetics ranking network with attributes and content adaptation," in *European Conference on Computer Vision (ECCV)*, 2016.

[12] X. Lu, Z. Lin, H. Jin, J. Yang, and J. Z. Wang, "Rapid: Rating pictorial aesthetics using deep learning," in *International Conference on Multimedia*. ACM, 2014, pp. 457–466.

[13] Y. Kao, R. He, and K. Huang, "Deep aesthetic quality assessment with semantic information," *IEEE Transactions on Image Processing*, vol. 26, no. 3, pp. 1482–1495, 2017.

[14] S. Ma, J. Liu, and C. Wen Chen, "A-lamp: Adaptive layout-aware multi-patch deep convolutional neural network for photo aesthetic assessment," in *Conference on Computer Vision and Pattern Recognition (CVPR)*. IEEE, 2017, pp. 4535–4544.

[15] S. Bianco, L. Celona, P. Napolitano, and R. Schettini, "Predicting image aesthetics with deep learning," in *International Conference on advanced concepts for intelligent vision systems*. Springer, 2016, pp. 117–125.

[16] V. Hosu, B. Goldlucke, and D. Saupé, "Effective aesthetics prediction with multi-level spatially pooled features," in *Conference on Computer Vision and Pattern Recognition (CVPR)*. IEEE, 2019, pp. 9375–9383.

[17] Y. Shu, Q. Li, S. Liu, and G. Xu, "Learning with privileged information for photo aesthetic assessment," *Elsevier Neurocomputing*, vol. 404, pp. 304–316, 2020.

[18] B. Pan, S. Wang, and Q. Jiang, "Image aesthetic assessment assisted by attributes through adversarial learning," in *AAAI Conference on Artificial Intelligence*, vol. 33, no. 01, 2019, pp. 679–686.

[19] H. Talebi and P. Milanfar, "Nima: Neural image assessment," *IEEE Transactions on Image Processing*, vol. 27, no. 8, pp. 3998–4011, 2018.

[20] X. Zhang, X. Gao, W. Lu, and L. He, "A gated peripheral-foveal convolutional neural network for unified image aesthetic prediction," *IEEE Transactions on Multimedia*, vol. 21, no. 11, pp. 2815–2826, 2019.

[21] Q. Chen, W. Zhang, N. Zhou, P. Lei, Y. Xu, Y. Zheng, and J. Fan, "Adaptive fractional dilated convolution network for image aesthetics assessment," in *Conference on Computer Vision and Pattern Recognition (CVPR)*, 2020, pp. 14 114–14 123.

[22] L. Marchesotti, F. Perronnin, D. Larlus, and G. Csurka, "Assessing the aesthetic quality of photographs using generic image descriptors," in *International Conference on Computer Vision (ICCV)*. IEEE, 2011, pp. 1784–1791.

[23] M. Leonardi, P. Napolitano, A. Rozza, and R. Schettini, "Modeling image aesthetics through aesthetic-related attributes," in *London Imaging Meeting*, vol. 2021, no. 1. Society for Imaging Science and Technology, 2021, pp. –.

[24] N. Murray, L. Marchesotti, and F. Perronnin, "Ava: A large-scale database for aesthetic visual analysis," in *Conference on Computer Vision and Pattern Recognition (CVPR)*. IEEE, 2012, pp. 2408–2415.

[25] Y. Deng, C. C. Loy, and X. Tang, "Image aesthetic assessment: An experimental survey," *IEEE Signal Processing Magazine*, vol. 34, no. 4, pp. 80–106, 2017.

[26] L. Zhang, Y. Gao, R. Zimmermann, Q. Tian, and X. Li, "Fusion of multichannel local and global structural cues for photo aesthetics evaluation," *IEEE Transactions on Image Processing*, vol. 23, no. 3, pp. 1419–1429, 2014.

[27] Y.-L. Hui, J. See, M. Kairanbay, and L.-K. Wong, "Multigap: Multi-pooled inception network with text augmentation for aesthetic prediction of photographs," in *International Conference on Image Processing (ICIP)*. IEEE, 2017, pp. 1722–1726.

[28] Y. Zhou, X. Lu, J. Zhang, and J. Z. Wang, "Joint image and text representation for aesthetics analysis," in *International Conference on Multimedia*. ACM, 2016, pp. 262–266.

[29] X. Lu, Z. Lin, X. Shen, R. Mech, and J. Z. Wang, "Deep multi-patch aggregation network for image style, aesthetics, and quality estimation," in *International Conference on Computer Vision (ICCV)*. IEEE, 2015, pp. 990–998.

[30] L. Mai, H. Jin, and F. Liu, "Composition-preserving deep photo aesthetics assessment," in *Conference on Computer Vision and Pattern Recognition (CVPR)*. IEEE, 2016, pp. 497–506.

[31] X. Zhang, X. Gao, L. He, and W. Lu, "Mscan: Multimodal self-and-collaborative attention network for image aesthetic prediction tasks," *Elsevier Neurocomputing*, vol. 430, pp. 14–23, 2021.

[32] F. Gao, Z. Li, J. Yu, J. Yu, Q. Huang, and Q. Tian, "Style-adaptive photo aesthetic rating via convolutional neural networks and multi-task learning," *Elsevier Neurocomputing*, vol. 395, pp. 247–254, 2020.

- [33] J.-T. Lee, C. Lee, and C.-S. Kim, "Property-specific aesthetic assessment with unsupervised aesthetic property discovery," *IEEE Access*, vol. 7, pp. 114 349–114 362, 2019.
- [34] V. Vapnik and A. Vashist, "A new learning paradigm: Learning using privileged information," *Elsevier Neural networks*, vol. 22, no. 5-6, pp. 544–557, 2009.
- [35] A. Benjamin, D. Rolnick, and K. Kording, "Measuring and regularizing networks in function space," in *International Conference on Learning Representations*, 2018.
- [36] J. Deng, W. Dong, R. Socher, L.-J. Li, K. Li, and L. Fei-Fei, "Imagenet: A large-scale hierarchical image database," in *Conference on Computer Vision and Pattern Recognition (CVPR)*. IEEE, 2009, pp. 248–255.
- [37] H. Lin, V. Hosu, and D. Saupe, "Deepfl-iqu: Weak supervision for deep iqa feature learning," *arXiv preprint arXiv:2001.08113*, 2020.
- [38] G. V. Reddy, S. Mukherjee, and M. Thakur, "Measuring photography aesthetics with deep cnns," *IET Image Processing*, vol. 14, no. 8, pp. 1561–1570, 2020.
- [39] M. Tan and Q. Le, "Efficientnet: Rethinking model scaling for convolutional neural networks," in *International Conference on Machine Learning*. PMLR, 2019, pp. 6105–6114.
- [40] G. C. Cupchik, "Emotion in aesthetics: Reactive and reflective models," *Poetics*, vol. 23, no. 1-2, pp. 177–188, 1995.
- [41] J.-T. Lee, H.-U. Kim, C. Lee, and C.-S. Kim, "Photographic composition classification and dominant geometric element detection for outdoor scenes," *Elsevier Journal of Visual Communication and Image Representation*, vol. 55, pp. 91–105, 2018.
- [42] S. Karayev, M. Trentacoste, H. Han, A. Agarwala, T. Darrell, A. Hertzmann, and H. Winnemoeller, "Recognizing image style." in *British Machine Vision Conference (BMVC)*, 2014.
- [43] D. P. Kingma and J. Ba, "Adam: A method for stochastic optimization," *arXiv preprint arXiv:1412.6980*, 2014.
- [44] G. Malu, R. S. Bapi, and B. Indurkha, "Learning photography aesthetics with deep cnns," *arXiv preprint arXiv:1707.03981*, 2017.
- [45] Z. Chen, "Data covariance learning in aesthetic attributes assessment," *Journal of Applied Mathematics and Physics*, vol. 8, no. 12, pp. 2869–2879, 2020.
- [46] L. Van der Maaten and G. Hinton, "Visualizing data using t-sne." *Journal of machine learning research*, vol. 9, no. 11, 2008.



Paolo Napolitano is associate professor at the University of Milano-Bicocca (Italy). In 2007, he received a PhD in Information Engineering from the University of Salerno (Italy). In 2003, he received a Master's degree in Telecommunications Engineering from the University of Naples Federico II. His current research interests focus on signal, image and video analysis and understanding, multimedia information processing and management and machine learning for multi-modal data classification and understanding.



Luigi Celona is currently a postdoctoral fellow at DISCo (Department of Informatics, Systems and Communication) of the University of Milano-Bicocca, Italy. In 2018 and 2014, he obtained respectively the PhD and the MSc degree in Computer Science at DISCo. In 2011, he obtained the BSc degree in Computer Science from the University of Messina. His current research interests focus on image analysis and classification, machine learning and face analysis.



Alessandro Rozza is the Chief Scientist of last-minute.com group. In 2011, he received a Doctor of Philosophy degree (PhD) in Computer Science from the Department of Scienze dell'Informazione, Università degli Studi di Milano. From 2012 to 2014 he was Assistant Professor at Università degli Studi di Napoli-Parthenope. From 2015 to 2017, he was head of research at Waynaut. His research interests include machine learning and its applications.



Marco Leonardi is a Ph.D. student in Computer Science at DISCo (Department of Informatics, Systems and Communication) of the University of Milano-Bicocca, Italy. In 2018 and 2016, he obtained respectively his Master Degree and Bachelor Degree in Computer Science at DISCo focusing on Image Processing and Computer Vision tasks. The main topics of his current research concern image memorability and machine learning.